The Effect of Composition on the Pressure-Induced HCP (ϵ) Transformation in Iron

P. M. GILES AND A. R. MARDER

The pressure-induced phase transformations in iron-rich Fe-Mn and Fe-Ni-Cr alloys were studied using an opposed diamond anvil high-pressure X-ray diffraction unit and a liquid-medium hydrostatic pressure apparatus. Transformations occurring with both increasing and decreasing pressure were studied. It was found that alloy additions of manganese and of nickel plus chromium significantly reduce the formation pressure of the hcp phase and can in some cases stabilize the phase enough to prevent it from transforming into some other phase during pressure release. All of the transformations are shown to be martensitic. Pressurization of prepolished surfaces, a large transformation pressure hysteresis, and the "abaric" formation of the ϵ phase establish the transformation as martensitic.

A phase change in iron occurring under dynamic (explosive) pressurization conditions has been detected at 130 kbar (1 kilobar = 14,504 psi) using electrical resistivity[1] and shock-wave propagation.[2] This phase change has also been studied under static pressure conditions using X-ray diffraction[3-7] and Mossbauer spectroscopy.[8,9] Takahashi and Bassett[4] have published a pressure-temperature phase diagram for pure iron which shows that increased temperature and pressure tend to stabilize the close-packed structures. Recently, it was reported that the bcc → hcp transformation in iron, which begins at 130 kbars, was a martensitic transformation with the equilibrium pressure, P_0, at 107 ± 8 kbar.[10]

Since the discovery of the transition of iron from a bcc to hcp structure, many investigators have examined the effect of alloying elements on this transition. The effects of Si, V, Co, Mo, C, Ni, Cr, and Mn on the bcc → hcp transition pressures in iron under dynamic pressurization conditions, have been documented in several studies.[11-15] Using electrical resistivity and X-ray diffraction, Blackburn *et al.*[16] have investigated the Fe-Ru system under static pressure application. The effect of nickel on the static high-pressure transformation in iron was investigated by Takahashi *et al.* using X-ray diffraction.[6] Of the several alloying additions studied, only Mn, Ni, and Ni-Cr additions were found to decrease the bcc → hcp transformation pressure in iron.

Loree *et al.*[12] have studied the effect of manganese on the bcc → hcp transformation in pure iron and have found that increasing the manganese content (up to 12 pct Mn) lowers the transition pressure to 50 kbar. Minshall, Zukas, and Fowler[11,30] and Gust and Royce[15] have examined the effect of combined additions of nickel and chromium on the hcp (ϵ) phase transformation induced by dynamic pressure. Their results show that combinations of the two alloy additions (Cr + Ni) lead to much lower transformation pressures than can be obtained with single alloy additions of the same amount.

The literature shows that manganese and nickel-chromium additions tend to stabilize the high-pressure hcp phase of iron.[12-13] However, since the results on these alloy additions were obtained from dynamic high-pressure measurements, the transformation finish, percentage transformed, the reverse transformations, and the structure of the resulting phase could not be determined. The study reported in the present paper has therefore utilized a static high-pressure X-ray technique to determine the effect of manganese and nickel-chromium on the phase stability of hcp iron.

EXPERIMENTAL PROCEDURES

All of the alloys used in this study were vacuum-induction melted, cast in vacuum, and hot-rolled to $\frac{3}{4}$ by 5 in. plates. All subsequent fabrication was done by machining. The compositions of the eight iron-based alloys are shown in Table I. The 1A to 1E series contains varying amounts of manganese, and the 2A and 2D samples are the Fe-Ni-Cr alloys. After filing each alloy to obtain a few grams of powder, the powder was annealed in evacuated Vycor capsules. The Fe-Mn alloys were annealed at 1800°F for one hour and furnace cooled, whereas the Fe-Ni-Cr alloys were annealed at 1900°F for 1 hr followed by an air cool. Bulk samples of the Fe-11.6 pct Ni-17.4 pct Cr alloy to be subjected to hydrostatic pressures were machined to 0.75 in. diam, ground flat and parallel to a thickness of 0.05 in., and vacuum-annealed at 1900°F for 1 hr followed by an air cool.

A schematic drawing of the high-pressure X-ray

Table I. Compositions of Alloys Studied at High Pressures*

Sample	C	Mn	P	S	Ni	Cr
1A	0.003	4.9	0.004	0.005	0.02	0.01
1B	0.004	9.6	0.001	0.006	0.03	0.02
1C	0.004	13.9	0.001	0.006	0.02	0.02
1D	0.002	17.7	0.001	0.006	0.03	0.05
1E	0.001	1.03	0.005	0.003	0.02	0.01
2A	0.005	<0.01	0.002	0.010	8.1	18.0
2B	0.004	<0.01	0.003	0.009	11.6	17.4
2C	0.003	<0.01	0.003	0.007	12.3	12.5
2D	0.002	<0.01	0.002	0.007	14.9	10.0

*Si, Mo, and V <0.01 and Al and Cu <0.003.

P. M. GILES and A. R. MARDER are Engineer and Supervisor, respectively, Alloy Development Section, Homer Research Laboratories, Bethlehem Steel Corp., Bethlehem, Pa.

Manuscript submitted November 10, 1969.

camera[17] used to obtain the high-pressure X-ray diffraction patterns is shown in Fig. 1. The unit consists essentially of a cylinder inside of which a piston is free to move. A flat-faced piston diamond is attached to one end of the piston, and a similar anvil diamond is attached to a demountable anvil assembly that is held in place by a backing plate during operation. The diameter of the anvil diamond face, 0.040 in., is approximately twice that of the piston diamond. The sample is placed between the two diamond surfaces. Pressure is applied to the sample using a known gas pressure on the back surface of the piston assembly. The gas is fed through a high-pressure gas line and pressure regulator attached to a tank of dry nitrogen. The high ratio–approximately 10,000 to 1–of the surface area of the back of the piston assembly to the surface area of the piston diamond face made it possible to generate the high pressures required to induce transformations in the specimen.

Phase-pressure information was obtained by taking a series of diffraction patterns as follows: for ambient and increasing pressures at 10 or 20 kbar increments up to a nominal pressure of 80 kbar; and for decreasing pressures, again at 10 to 20 kbar increments, down to ambient pressure. Transformation pressures and percentages of phases present were noted as a function of nominal pressure. The diffraction patterns were then measured and interplanar spacing calculated. The actual pressures were arrived at by using a calibration curve of the unit which was derived by substituting experimentally determined lattice parameters of iron into the equation developed by Mao *et al.*[5] A 0.003 in. beam size was used in the iron experiments.

Some larger samples—0.75 in. diam by 0.050 in.—were subjected to hydrostatic (liquid medium) pressurization in a commercial piston and cylinder device capable of achieving pressures up to 30 kbar. Similar type of equipment is described by Davidson and Homan.[18]

RESULTS AND DISCUSSION

The effect of manganese additions on the bcc → hcp and hcp → bcc transformation pressures in pure iron will first be described. The effect of additions of nickel plus chromium on the transformation pressures and phases will then be discussed. Finally, these results will be reviewed in the light of the characteristics of a martensitic transformation, and the results substantiating this type of transformation will be presented.

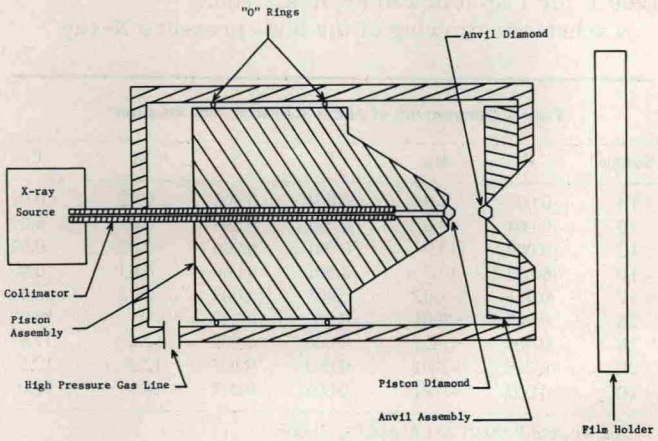

Fig. 1—Schematic of high-pressure X-ray diffraction camera.

Iron-Manganese

Table II shows the percentage of phases present for the four Fe-Mn alloys at 0, 25, and 155 kbar as pressure was increased and at ambient pressure after all pressure was released. The phase contents of the annealed samples—which appear in the left-hand 0 kbar column—agree with the values presented by Schumann.[19-20] The table shows that manganese additions tend to increase the amount of hcp phase formed at a given pressure and to increase the stability of this phase. Fig. 2 is a plot of the transition pressure (the pressure at which a change in the amount of phases present began) vs the manganese content of the samples. The upper solid curve is for the beginning of the bcc → hcp transformation ($P_{M_s}^{\alpha\rightarrow\epsilon}$) during increasing pressure. The data of Loree *et al.*[12] is also included in this figure and shows excellent agreement with these results. The lower solid curve is for the beginning of the reverse transformation ($P_{M_s}^{\epsilon\rightarrow\alpha}$) which occurred during decreasing pressure. All samples were pressurized to approximately 80 kbar nominal pressure (160 kbar actual) before the decreasing pressure diffraction patterns were obtained. As shown in Table II, the tendency of increased manganese additions to promote the formation of the hcp phase is clearly demonstrated by the decreasing transformation pressures. In the case of both the Fe-13.9 pct Mn and the Fe-17.7 pct Mn alloy, none of the hcp formed at high pressure transformed back to bcc as pressure was released, thus resulting in a 100 pct hcp structure at ambient pressure.

Fig. 3 shows five of a series of fifteen diffraction patterns obtained from an Fe-4.9 pct Mn alloy at the pressures shown in kbar next to each pattern. The arrows indicate increasing or decreasing nominal pressure and were obtained in the order going from top to bottom. The numbered vertical lines running between the patterns indicate the approximate positions of the diffraction lines which are identified in the table below the patterns. It can be seen that the sample is 100 pct bcc at 30 kbar nominal pressure (55 kbar actual pressure), and begins to transform to hcp at 40 kbar nominal pressure (90 kbar actual). This is shown by the fact that lines 1 and 3 first appear at 40 kbar nominal pressure and by the increase in intensity of these lines up to 80 kbar nominal pressure. The transforma-

Table II. Phases Present in Fe-Mn Alloys at Various Pressures

Sample	Pct Mn	Phase	Pct of Phase Present at: 0 Kbar	25 Kbar	155 Kbar	0 Kbar
1A	4.9	α	100	100	70	95
		ϵ	0	0	30	5
1B	9.6	α	100	100	50	70
		ϵ	0	0	50	30
1C	13.9	α	95	100	0	5
		ϵ	5	0	100	95
1D	17.7	α	0	0	0	0
		γ	50	50	0	0
		ϵ	50	50	100	100

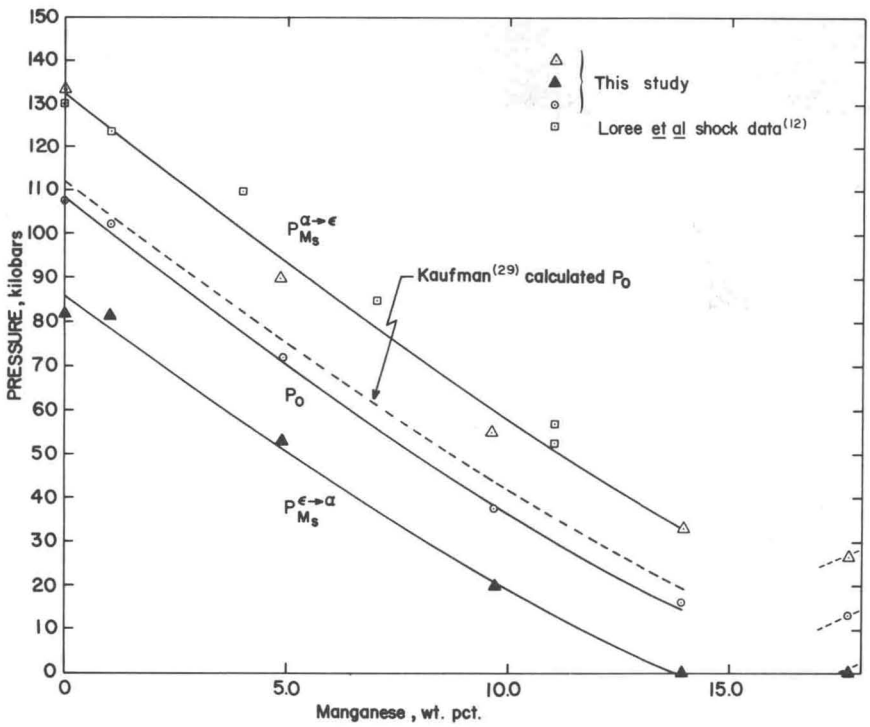

Fig. 2—Effect of manganese on the transformation pressures of iron.

tion back to bcc as the pressure is reduced is evidenced by the low intensity of the 1 and 3 lines at 0 kbar. These diffraction patterns clearly demonstrate: a) the bcc $\rightleftarrows$ hcp nature of the transformation, b) the gradual increase in the amount of the hcp phase as pressure is increased, and c) the transformation of most of the hcp back to bcc as pressure was released.

In the case of the Fe-17.7 pct Mn sample, this basic transformation pattern exhibits some interesting variations. This sample initially has a structure which is about 50 pct fcc and 50 pct hcp in the annealed condition. The diffraction pattern in Fig. 4 (Fe-17.7 pct Mn alloy) taken at 18 kbar nominal pressure (33 kbar actual pressure) shows this untransformed crystallographic structure. The data show that the transformation starts at 26 kbar actual pressure. In Fig. 4, the increase in the intensity of the number three line (1.92Å-hcp) at 30 kbar nominal pressure (47.5 kbar actual pressure) indicates that the transformation then proceeds as pressure is increased until the sample is 100 pct hcp at 50 kbar nominal (120 kbar actual). Upon release of pressure, the hcp structure is retained. Since the sample contains no bcc prior to the beginning of transformation, the transformation which occurs is either a $\gamma \rightarrow \epsilon$ transformation or is due to a $\gamma \rightarrow (\alpha) \rightarrow \epsilon$ type transformation where the fcc first shears to bcc. This bcc then transforms immediately to hcp because the bcc is unstable at this pressure. The necessary $\gamma \rightarrow \alpha \rightarrow \epsilon$ martensitic transformation associated with deformation has been proposed for stainless steels[21-22] and Schumann[19] has observed both a $\gamma \rightarrow \alpha$ and $\gamma \rightarrow \epsilon$ martensitic transformation in Fe-Mn alloys containing 0 to 10, and 14.5 to 27 pct manganese, respectively.

As in the case of pure iron,[10] the transformations for the Fe-Mn alloys are "abaric," *i.e.*, the extent of completion of the transformation is determined by the difference between the applied pressure and the pressure necessary to initiate the transformation. Also, there is a hysteresis between the pressures required to initiate the forward and reverse transformations. These observations again indicate that the transformation may be of the martensitic type.

Plotted in Fig. 2 is a P_0 curve, or the equilibrium $\alpha \rightleftarrows \epsilon$ transformation line, determined from the following equation:[10]

$$P_0 = \frac{P_{M_s}^{\alpha\to\epsilon} + P_{M_s}^{\epsilon\to\alpha}}{2} \qquad [1]$$

This equation is the analogue of the Kaufman and Cohen[24] equilibrium temperature equation, T_0, derived for the martensite transformation. Also shown in Fig. 2 is the calculated P_0 line for Fe-Mn alloys.[29] This line was determined from the free energy equation:

$$\Delta F^{\alpha\to\epsilon}[T_1 P_1 x] = (1-x)\Delta F_{\mathrm{Fe}}^{\alpha\to\epsilon} + x\Delta F_{\mathrm{Mn}}^{\alpha\to\epsilon} + x(1-x)(E-A)_{\mathrm{FeMn}} + 23.9 P \Delta V^{\alpha\to\epsilon} \qquad [2]$$

where x = atomic fraction Mn

at 300°K $\Delta F_{\mathrm{Fe}}^{\alpha\to\epsilon} = +1010$ cal per g-atom

$\Delta F_{\mathrm{Mn}}^{\alpha\to\epsilon} = +1080$ cal per g-atom

interaction parameter $(E-A) = -6990$ cal per g-atom

$\Delta V^{\alpha\to\epsilon} = -0.38$ cu cm per g-atom

Substituting in Eq. [2]:

$$\Delta F^{\alpha\to\epsilon}[300, P_0, x] = 0 = (1-x)1010 + x(1080) + x(1-x)(-6990) - 9.082 P_0 \qquad [3]$$

or,

$$P_0 \approx 111.2 - 763x + 769x^2 \qquad [4]$$

It can be seen that there is substantial agreement be-

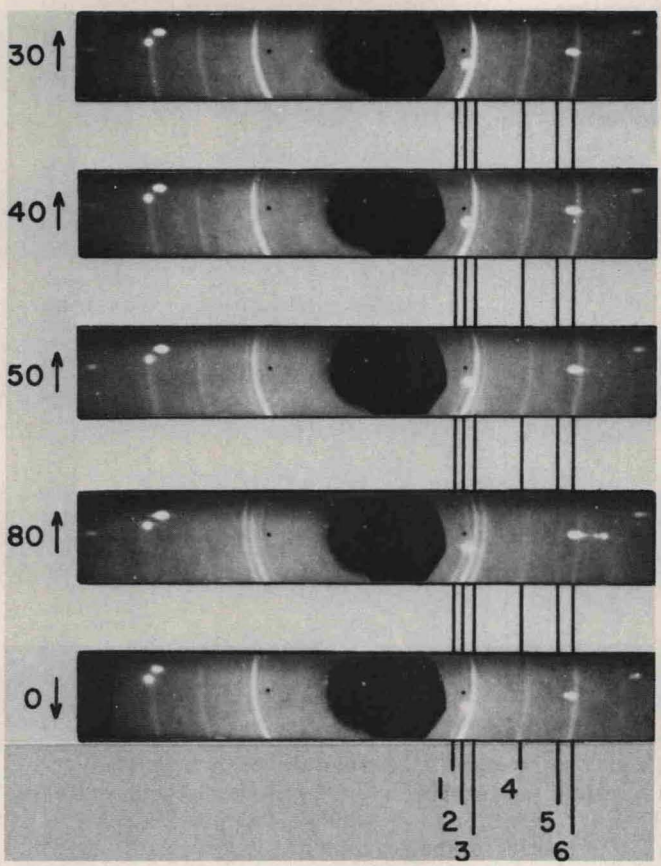

Line	Interplanar Spacing, Å	Phase and Indices		
1	2.17		$\epsilon(100)$	
2	2.04	$\alpha(110)$	$\epsilon(002)$	$\gamma(111)$
3	1.92		$\epsilon(101)$	
4	1.43	$\alpha(200)$		
5	1.25		$\epsilon(110)$	$\gamma(220)$
6	1.17	$\alpha(211)$		

Fig. 3—High-pressure X-ray diffraction patterns with diffraction lines identified. Sample was iron-4.9 pct manganese. Nominal pressures are given to the left of each diffraction pattern. Arrows pointing up show increasing pressure and arrows pointing down show decreasing pressures.

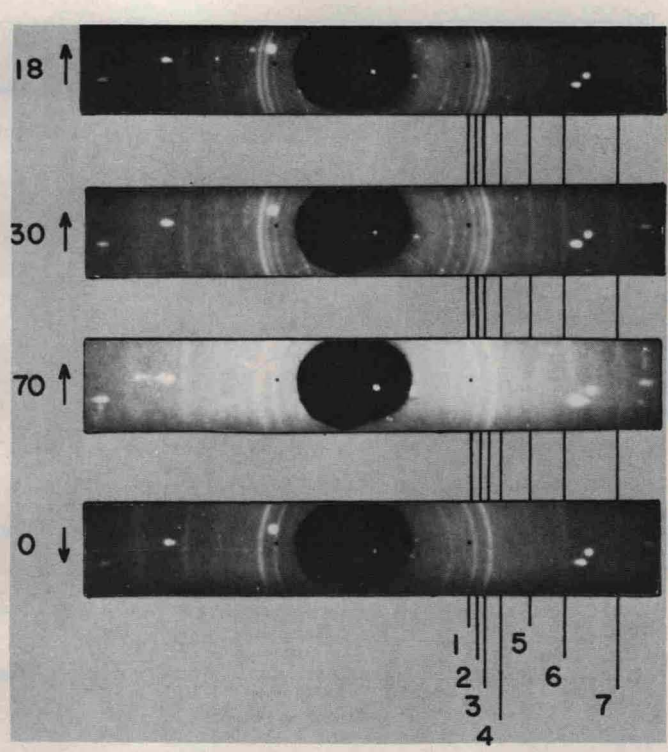

Line	Interplanar Spacing, Å	Phase and Indices		
1	2.17		$\epsilon(100)$	
2	2.04	$\alpha(110)$	$\epsilon(002)$	$\gamma(111)$
3	1.92		$\epsilon(101)$	
4	1.79			$\gamma(200)$
5	1.48		$\epsilon(102)$	
6	1.25		$\epsilon(110)$	$\gamma(220)$
7	1.08		$\epsilon(112)$	$\gamma(311)$

Fig. 4—High-pressure X-ray diffraction patterns with diffraction lines identified. Sample was iron-17.7 pct manganese. Nominal pressures are given to the left of each diffraction pattern. Arrows pointing up show increasing pressure and arrows pointing down show decreasing pressure.

tween the calculated and the experimentally determined P_0. Furthermore, the driving force for the bcc → hcp martensite transformation, calculated by multiplying the difference in pressure between $P_{M_s}^{\alpha\rightarrow\epsilon}$ and P_0 by $23.9\Delta V$, ranges from 227 cal per g-atom at 0 pct Mn[10] to 150 cal per g-atom at 13.9 pct Mn. This is in good agreement with determined values of 150 to 300 cal per g-atom calculated for the martensite transformation in iron alloys.[24]

Iron-Nickel-Chromium

The compositions of the Fe-Ni-Cr alloys studied (Table I, series 2A to 2D) were chosen to correspond closely to the composition of alloys which Minshall, Zukas, and Fowler[11,30] found to have low transformation pressures. Their transformation pressures were determined by means of dynamic pressurization and could not determine the structure of the phase formed at high pressure or the pressure at which it began to return to the ambient-pressure phase during pressure release. Also, the alloy compositions selected are close to those of some grades of stainless steels. The transformations in these materials are of considerable commercial importance, and several papers are available that deal with the transformations in such alloys under conditions of varying thermomechanical processes.[21-23,25-27]

Table III shows the percentage of phases present for these alloys at 0, 25, and 155 kbar as pressure was increased and at ambient pressure after all pressure was released. It can be seen that γ as well as α and ϵ phases are present in these alloys and that the transformations begin at much lower pressures than were observed in the Fe-Mn alloys. It is also evident that the 11.6 pct Ni-17.4 pct Cr alloy and the 12.3 pct Ni-13.5 pct Cr alloy retain their high pressure structure after pressure is released. This demonstrates that combined nickel and chromium additions promote the formation and stability of the hcp phase.

In Fig. 5, the combined alloying effects of Ni + Cr on the $\alpha \rightarrow \epsilon$ martensitic transformation of iron are plotted using the results of this investigation as well as the data of Fowler *et al.*[11,30] and Gust and Royce.[15] A smooth curve has been drawn through the data from

the high pressure martensitic transformation of pure iron at 133 kbar to a Ni + Cr content of 29.85 pct reported to be all austenitic.[15] This alloy did not undergo the $\alpha \rightarrow \epsilon$ transformation. From the figure it is seen that at the low Ni + Cr additions even the Fe-Ni and Fe-Cr data fit the curve. Beyond approximately 10 pct (Ni + Cr) deviations from the curve in the binary alloys occur and a synergistic effect of the combination of both nickel and chromium is evident. At the present time, this combined Ni + Cr effect on the transformation cannot be explained. Some deviation from the curve of the Gust and Royce data[15] is also noted and is unexplainable. However, a general trend is established showing that combined alloying additions of Ni + Cr lower the pressure of the $\alpha \rightarrow \epsilon$ transformation.

From reported measurements of stacking fault energy in Fe-Ni-Cr alloys,[28] it appears that a decrease in the stacking fault energy is not the cause of this strong interaction effect. A decrease in the stacking fault energy would promote the formation of hcp, at least from fcc. Dulieu and Nutting[28] show that increasing the nickel content of an Fe-18 pct Cr alloy increases the stacking fault energy, whereas pressure-transformation measurements show that the formation pressure of the hcp phase decreases rapidly with nickel additions in this composition range.

As in the results of the iron-manganese experiments, the extent of the $\alpha \rightarrow \epsilon$ and $\epsilon \rightarrow \alpha$ transformations is a function of the difference between the applied pressure and the initial formation pressure (they are abaric processes). The transformations also exhibit a difference between the pressure at which the forward and reverse transformations begin. This would again indicate that the transformation is martensitic in nature.

Table III. Phases Present in Fe-Ni-Cr Alloys at Various Pressures

Composition				Pct of Phase Present at:			
Sample	Pct Ni	Pct Cr	Phase	0 Kbar	25 Kbar	155 Kbar	0 Kbar
2A	8.1	18.0	α	0	95	40	70
			ϵ	0	5	60	30
			γ	100	0	0	0
2B	11.6	17.4	α	0	80	20	20
			ϵ	0	10	80	80
			γ	100	10	0	0
2C	12.3	12.5	α	0	50	20	20
			ϵ	0	0	80	80
			γ	100	50	0	0
2D	14.9	10.0	α	0	80	30	80
			ϵ	0	0	70	20
			γ	100	20	0	0

Martensite Transformation

To find out whether the transformation occurring in these alloys was martensitic, a large (0.75 in. diam by 0.050 in. thick) sample of Fe-11.6 pct Ni-17.4 pct Cr was exposed to a purely hydrostatic stress environment. This alloy was chosen because the hydrostatic pressure unit used in these experiments was limited to about 25 kbar. Thus, if the sample began to trans-

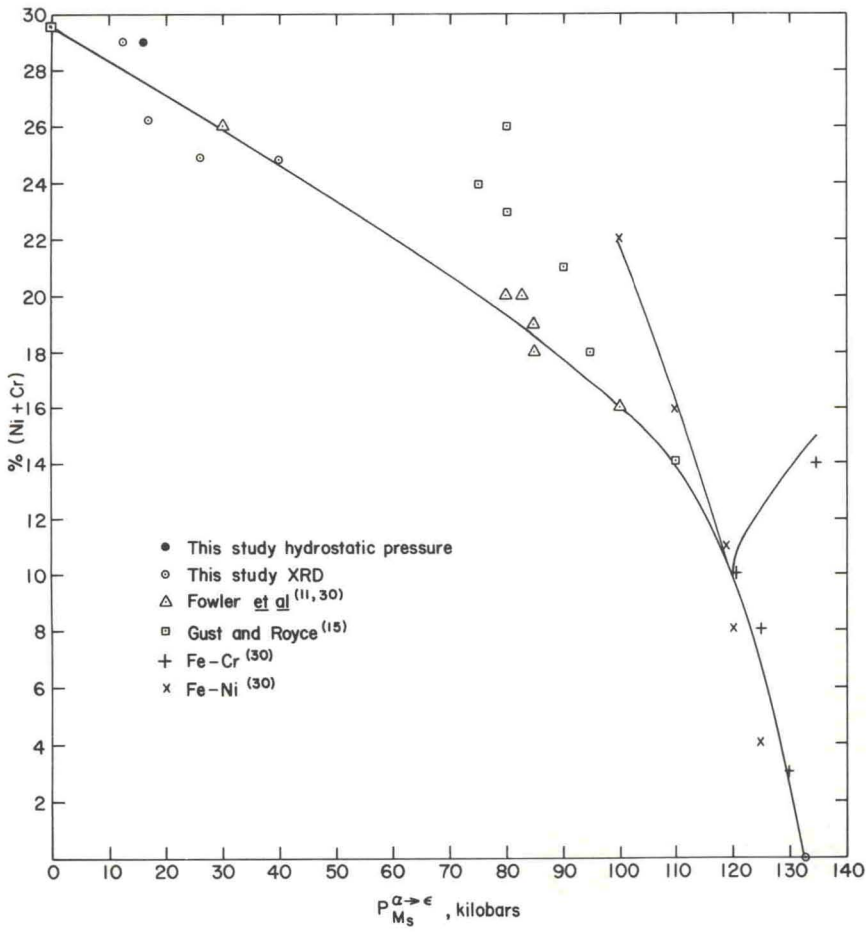

Fig. 5—The effect of Ni + Cr additions on the $\alpha \rightarrow \epsilon$ martensite transformation pressure.

form at 15 kbar—the hcp formation pressure of this alloy and the lowest observed during the program—the 10 kbar "overpressure" available would cause the formation of enough hcp martensite to permit a metallographic study of the hcp phase and, possibly, a study of its relation to both the bcc martensite and the fcc parent phase.

An annealed sample of the material was subjected to the following investigation schedule:

1) Polish and etch in 50 pct aqua regia-50 pct water
2) Photograph in incident light, Fig. 6(*a*)
3) Polish
4) Photograph in oblique light, Fig. 6(*b*)
5) X-ray
6) Pressurize to 25.5 kbar
7) X-ray
8) Photograph in oblique light, Figs. 6(*c*) and 7
9) Etch in 50 pct aqua regia-50 pct water
10) Photograph in incident light, Fig. 6(*d*).

All of the photographs in Fig. 6 are of the same area and were taken at 100× (reduced to magnification 85 times). Fig. 7 is a photomicrograph taken at 500× (reduced to magnification 375 times). The area shown in Fig. 7 is outlined in Fig. 6(*c*). This series of photographs showing the shear and shape change associated with the transformation clearly demonstrates the martensitic nature of the high-pressure transformation. X-ray diffraction showed that the pressurized sample consisted of: the fcc parent, about 15 pct hcp, and 5 pct bcc. All of the phases gave diffraction lines corresponding to the same interplanar spacing as the phases formed during pressurization in the high-pressure X-ray diffraction camera.

After repolishing of the distorted as-pressurized surface and etching with an aqueous solution of hydrochloric acid, ammonium bifluoride, and potassium metabisulfite, the 1000× photographs (reduced to magnification 740 times) appearing in Fig. 8 were obtained. The orthogonal-appearing transformation product bounded by straight, parallel sides shown in Fig. 8(*a*) was much more common that the acicular type of structure shown in Fig. 8(*b*). These structures are typical of those found for Fe-Mn and Fe-Ni-Cr alloys.[19,23] However, the metallographic distinction between the bcc and hcp phases has not been definitely established. The white matrix is fcc.

The relatively small amount (about 5 pct) of bcc phase observed by X-ray diffraction in the hydrostatically pressurized sample was quite surprising. Since the observation from the opposed-anvil X-ray diffraction patterns indicated that the bcc phase appears prior to the formation of the hcp as a deformation-induced structure, it was expected that the bcc material should constitute a larger portion of the sample than was ob-

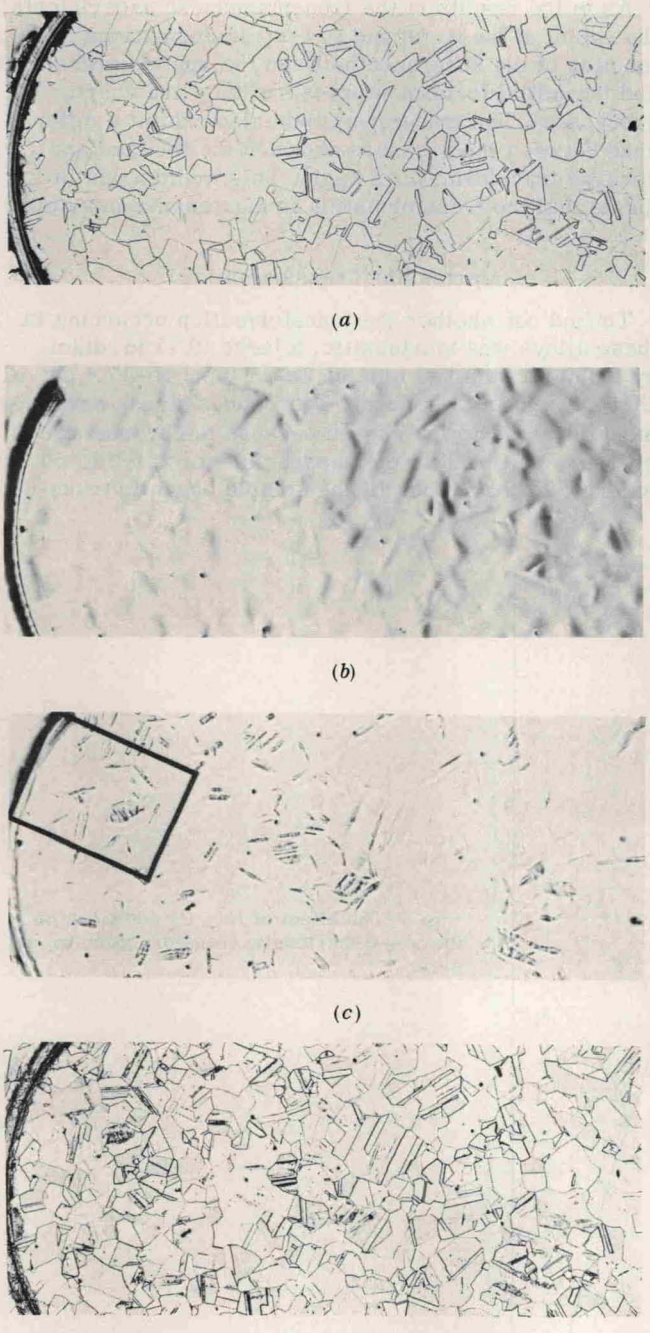

(*a*)

(*b*)

(*c*)

(*d*)

Fig. 6.—Fe-11.6 pct Ni-17.4 pct Cr before—(*a*) and (*b*)—and after—(*c*) and (*d*)—pressurization. (*a*) etched—incident light, (*b*) polished—oblique light, (*c*) polished—oblique light, (*d*) etched—incident light. Magnification 85 times.

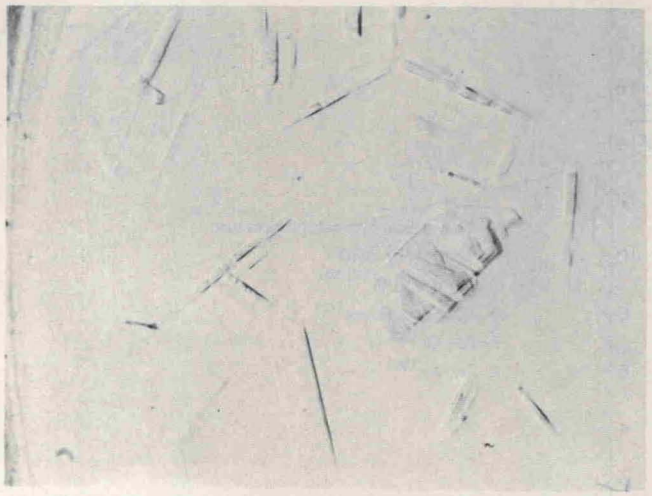

Fig. 7—Fe-11.6 pct Ni-17.4 pct Cr alloy after pressurization. The area is that outlined in Fig. 6(*c*). Oblique light. Magnification 375 times.

served and should form at a lower pressure than the hcp phase. To determine the accuracy of this hypothesis, a sample of annealed Fe-11.6 pct Ni-17.4 pct Cr was metallographically polished, X-rayed, and subjected to a series of pressurizations ranging from 7.5 to 25.5 kbar in 2.5 kbar intervals. Between each pressurization, the sample was X-rayed and observed microscopically. The sample was photographed when required for quantitative light metallography. Fig. 9 is a plot of the percentage of martensite in the sample vs the hydrostatic pressure. The data point at 17.5 kbar is based on a visual microscope estimate while those at 20.0, 22.5, and 25.5 kbar are based on quantitative light metallography. It was found that X-ray determination of the percentage of phases present was not accurate enough to be used because of a preferred orientation in the fcc parent phase that led to a preferred orientation in the hcp and bcc transformation products. X-ray diffraction of the samples revealed that no bcc martensite formed prior to the formation of the hcp martensite and that the amount of bcc structure formed was equal to approximately one-third the amount of hcp. From these observations, it appears that under purely hydrostatic stress the fcc phase transforms simultaneously into hcp and bcc martensite in an abaric manner.

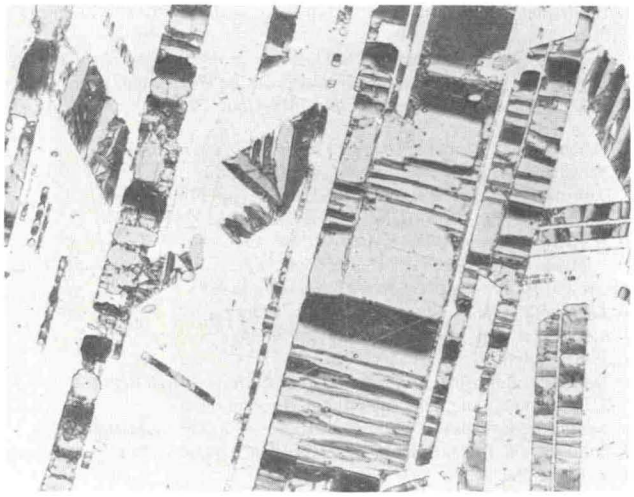

(*a*)

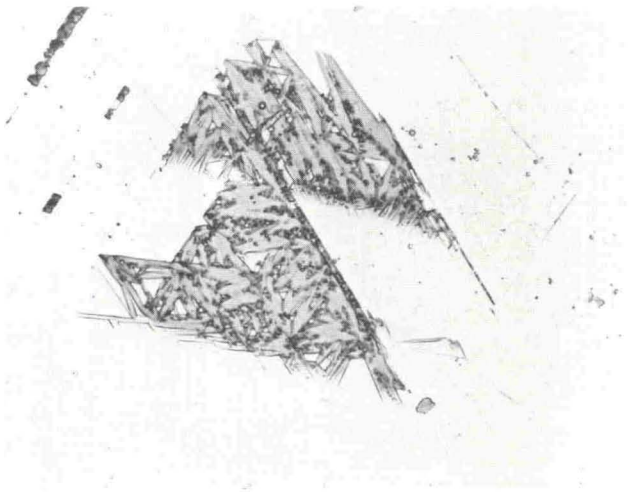

(*b*)

Fig. 8—Fe-11.6 pct Ni-17.4 pct Cr alloy subjected to 25.5 kbar. The figures show the two different structures found in the sample. (*a*) Magnification 740 times, (*b*) magnification 740 times.

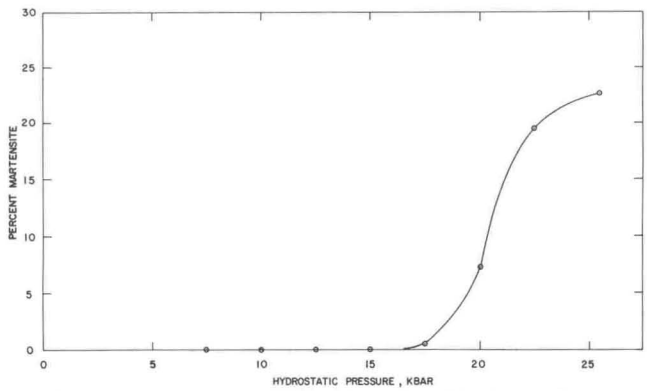

Fig. 9—Percent martensite as a function of hydrostatic pressure for Fe-11.6 pct Ni-17.4 pct Cr.

Two other observations were made regarding the nature of these transformations. First, microprobe analysis indicated no composition difference between the matrix and the transformation product. This is another prerequisite for a martensitic transformation. Second, it was found that the hcp martensite was metastable at ambient conditions. On heating to a temperature as low as 100°C, all of the hcp phase present transformed to the fcc phase. At these temperatures, the amount of bcc martensite remained constant.

The high-pressure transformation experiments undertaken in Fe-Ni-Cr alloys during this study have shown that the bcc → hcp, fcc → hcp, and hcp → bcc transformation pressures are composition-dependent and that the transformation is martensitic in nature.

CONCLUSIONS

X-ray diffraction and light metallographic examinations of phase transformations induced in iron-rich Fe-Mn and Fe-Ni-Cr alloys by means of high pressure showed that:

1) Alloy additions of manganese and of nickel plus chromium significantly reduce the formation pressure of the hcp phase and can in some cases stabilize the phase enough to prevent it from transforming into some other phase during pressure release.

2) All of the transformations are martensitic, as demonstrated by the following observations:

a) The transformation pressures do not represent equilibrium pressures because a hysteresis exists, *i.e.*, there is a difference between the forward and reverse transformation pressures.

b) The extent of the transformation is a function of the difference between the applied pressure and the pressure at which the phase first forms and is not a function of time at the applied pressure.

c) There is no difference in composition between the matrix and the transformation product.

d) Surface relief was observed on samples polished prior to pressurization.

ACKNOWLEDGMENTS

The authors would like to take this opportunity to acknowledge the technical assistance of R. E. Steiger-

walt, J. R. Gruver for electron microscopy; J. C. Hlubik for hydrostatic pressurization; J. R. Kilpatrick for metallography; and M. H. Longenbach for X-ray diffraction. The authors would also like to acknowledge the discussions and comments of H. Abrams and B. L. Bramfitt, the assistance of B. S. Mikofsky in the preparation of this manuscript, and L. Kaufman of ManLabs, Inc. for review of the manuscript.

REFERENCES

1. A. Balchan and H. G. Drickamer: *Rev. Sci. Instr.*, 1961, vol. 32, pp. 308-13.
2. D. Brancroft, E. L. Peterson, and S. Minshall: *J. Appl. Phys.*, 1956, vol. 27, pp. 291-98.
3. J. C. Jamieson and A. W. Lawson: *J. Appl. Phys.*, 1962, vol. 33, pp. 776-80.
4. T. Takahashi and W. A. Bassett: *Science*, 1964, vol. 145, pp. 483-86.
5. H-K Mao, W. A. Bassett, and T. Takahashi: *J. Appl. Phys.*, 1967, vol. 38, pp. 272-76.
6. T. Takahashi, W. A. Bassett, and H-K Mao: *J. Geophys. Res.*, 1968, vol. 73, pp. 4717-25.
7. R. L. Clendenen and H. G. Drickamer: *J. Phys. Chem. Solids*, 1964, vol. 25, p. 483.
8. D. M. Pipkorm, C. K. Edge, P. DeBrunner, G. DePasquali, H. G. Drickamer, and H. Frauenfelder: *Phys. Rev.*, 1964, vol. 135, pp. A1604-12.
9. L. E. Millet and D. L. Decker: *Phys. Lett.*, 1969, vol. 29A, p. 7.
10. P. M. Giles, M. H. Longenbach, and A. R. Marder: A High Pressure X-ray Diffraction Study of Iron, to be published in *J. Appl. Phys.*
11. F. S. Minshall, E. G. Zukas, and C. M. Fowler: Referenced by R. G. McQueen in *Metallurgy at High Pressures and High Temperatures*, K. Gschneider, N. A. D. Parlee, and M. T. Hepworth, eds., p. 76, Gordon and Breach Science Publishers, New York, 1964.
12. T. R. Loree, R. H. Warnes, E. G. Zukas, and C. M. Fowler: *Science*, 1966, vol. 153, pp. 1277-78.
13. T. R. Loree, C. M. Fowler, E. G. Zukas, and F. S. Minshall: *J. Appl. Phys.*, 1966, vol. 37, pp. 1918-27.
14. F. P. Bundy: *J. Appl. Phys.*, 1967, vol. 38, pp. 2446-49.
15. W. H. Gust and E. G. Royce: University of California, UCRL-50581, February 1969.
16. L. D. Blackburn, L. Kaufman, and M. Cohen: *Acta Met.*, 1965, vol. 13, pp. 533-41.
17. C. E. Weir, A. VanValkenberg, and E. Lippincott: in *Modern Very High Pressure Techniques*, R. H. Wentorf, ed., p. 51, Butterworths, Washington, 1962.
18. T. E. Davidson and C. G. Homan: *Trans. TMS-AIME*, 1963, vol. 227, pp. 167-76.
19. H. Schumann: *Arch. Eisenhuettenw.*, 1967, vol. 38, pp. 647-51.
20. H. Schumann: *Neue Huette*, 1968, vol. 13, pp. 479-82.
21. J. Dash and H. M. Otte: *Acta Met.*, 1963, vol. 11, pp. 1169-78.
22. J. F. Breedis: *Trans. TMS-AIME*, 1964, vol. 230, pp. 1583-96.
23. P. M. Kelly: *Acta Met.*, 1965, vol. 13, pp. 635-46.
24. L. Kaufman and M. Cohen: *Progress in Metal Physics*, B. Chalmers and R. King, eds. vol. 7, pp. 165-246, Pergamon Press, London 1958.
25. R. Lagneborg: *Acta Met.*, 1964, vol. 12, pp. 823-43.
26. J. A. Venables: *Phil. Mag.*, 1962, vol. 7, pp. 35-44.
27. R. P. Reed: *Acta Met.*, 1962, vol. 10, pp. 865-77.
28. D. Dulieu and J. Nutting: *Brit. Iron and Steel Institute Special Report* #86, p. 143, Percy Lund, Humphries and Co. Ltd., London, 1964.
29. L. Kaufman: ManLabs Inc., Cambridge, Mass., private communications (See J. F. Breedis and L. Kaufmann: *Formation of HCP and BCC Phases in Austentic Iron Alloys, Met. Trans.*, 1971, in press).
30. C. M. Fowler, F. S. Minshall and E. G. Zukas: *Response of Metals to High Velocity Deformation*, P. G. Shewmon and V. F. Zackay, eds., pp. 275-341, Interscience, New York, 1961.